

Surgical anatomy of the infratemporal fossa using the transmaxillary approach

P.-H. Roche, H.-D. Fournier, L. Laccourreye and Ph. Mercier

Laboratoire d'Anatomie, Faculté de médecine, rue haute de reculée, F-49045 Angers cedex, France

Received October 30, 2000 / Accepted in final form March 28, 2001

Key words: Cranial base surgery - Infratemporal fossa - Maxillary sinus - Pterygopalatine fossa - Surgical anatomy

Correspondence to: Ph.Mercier

E-mail: philippe.mercier@univ-angers.fr

Abstract

Abstract In this study we evaluated the ability of the transmaxillary route to expose the elements of the infratemporal fossa (ITF). Five adult cadaver heads were dissected on both sides, after making a paralateronasal incision. The maxillary branch of the trigeminal nerve served as a superior landmark to progress into the retroantral space and pterygopalatine fossa. The maxillary artery, lateral pterygoid muscle, pterygoid venous plexus, foramen rotundum and foramen ovale were identified. Distances between those elements and angle of approaches of the foramen ovale and foramen rotundum were measured in the horizontal plane. In all cases, the anterior loop of the maxillary artery and the sphenopalatine artery were located in the proximal retroantral fatty space and could be ligated without optic magnification. The maxillary nerve could be followed up to the foramen rotundum at a 44 mm mean distance from the opening. The mean angle of vision to the foramen rotundum was 31°. Under the greater sphenoid wing and lateral to the pterygoid process, desinsertion and partial resection of the lateral pterygoid muscle were required to identify the pterygoid venous plexus and foramen ovale. The pterygoid venous plexus was organized as a compact network of channels between and superior to the muscle fibers it was in close relation with the foramen ovale. Access to the foramen ovale was deep (mean 56 mm) and narrow (20°). Our results indicate that the transmaxillary approach is a minimally invasive procedure that gives an appropriate window to the structures of the retroantral space and to the pterygomaxillary fissure and pterygopalatine fossa. Monitoring of the retropterygoid portion of the infratemporal fossa by this route is inadequate.

Numerous approaches have been recommended for exposure of the infratemporal fossa (ITF). Management of lesions involving the ITF remains challenging because it often requires extensive procedures, a source of cosmetic and functional complications. Among the conservative approaches, the transmaxillary route was early recommended for ligation of the maxillary a. (MA) in cases of severe epistaxis. Recently, some authors have reconsidered the value of this route for the control of deeper located structures, such as the anterior part of the cavernous sinus [2].

The aim of the present anatomic study was to determine the limits of exposure of the elements of the ITF, via the transmaxillary approach.

Materials and methods

For this study, 5 adult cadaver heads (10 specimens) were dissected by using both macro - and microsurgical techniques and instrumentation. Optic magnifications used were x 6 to x 40. Colored latex was injected into the vascular structures to facilitate their definition in three specimen cadavers. The trajectory of the dissection is materialized in Figs. 1 and 2.

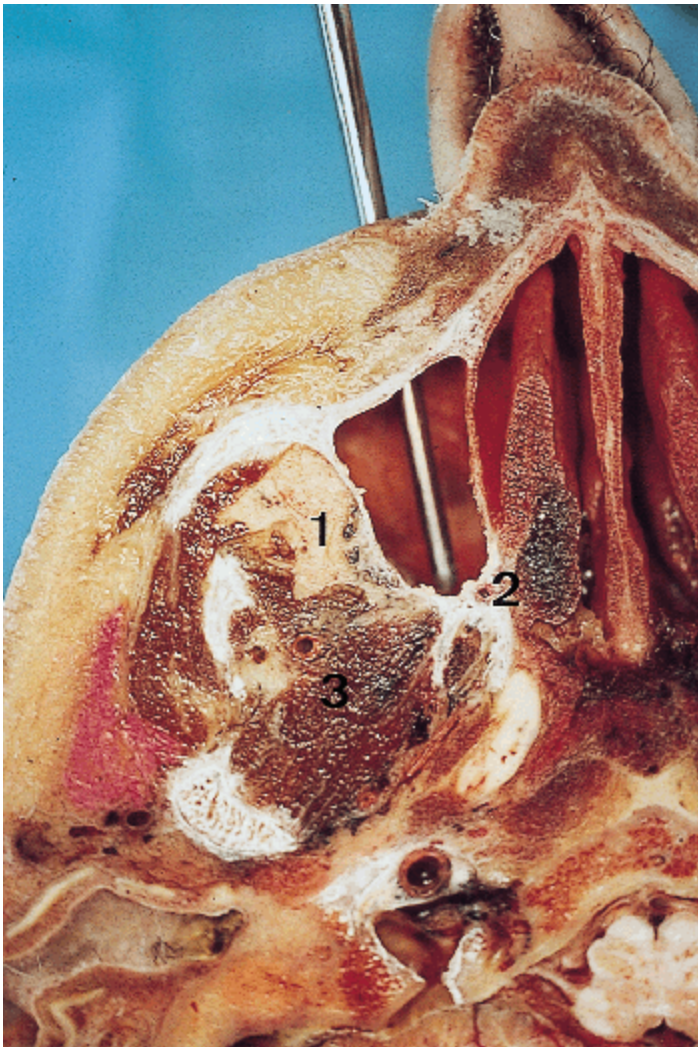


Fig. 1 Inferior view of an axial frozen section through the plan of the right maxillary antrum and simulation of the transmaxillary approach. The tip of the cannula reaches the posterior wall of the maxilla, in close relationship with the anterior part of the pterygoid process. The three sub-regions of the infratemporal fossa are clearly identified. 1, retromaxillozygomatic area 2, pterygopalatine fossa 3, pterygoid mm.



Fig. 2 Lateral view of a sagittal frozen section through the plan of the maxillary antrum (1). The posterior wall of the maxilla and the pterygoid process (2) are colored in white. These bony structures delineate medially the area of the pterygopalatine fossa (3). Behind the pterygoid plate, the area just under the foramen ovale (4) is clearly exposed

Antromaxillary stage

A paralateronasal skin incision was done, extending vertically from the medial canthal region to the upper lip, as described in transfacial approaches. A subperiosteal dissection of the soft tissues exposed the anterior surface of the maxilla up to the level of the infra-orbital foramen. Identification of this latter structure allowed us to identify, spare and gently retract the infraorbital n. and a. superiorly and laterally (Fig. 3). An oblique quadrangular osteotomy of the anterior wall of the maxilla (a thin shell of bone) was performed, providing a 6 cm-square window in the antrum (Fig. 4). After removal of the mucosa, the course of the infraorbital n. could be identified because of the very thin and translucent consistency of the floor of the infraorbital canal.

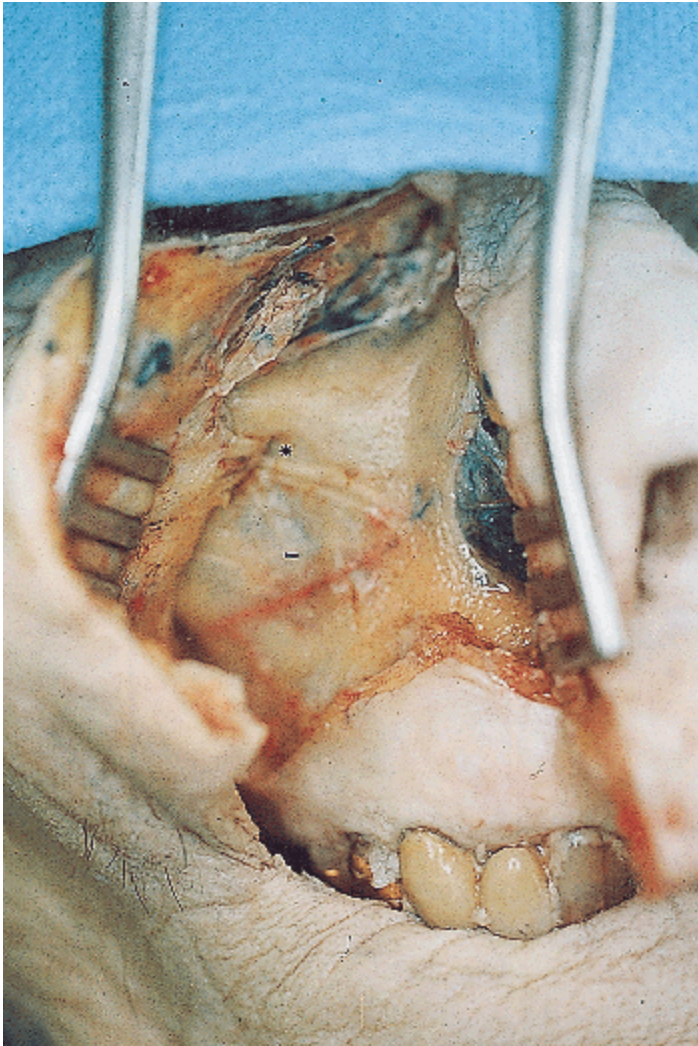


Fig. 3 Surgical anatomy of the first stage of the approach (right side). The paralateronasal skin incision, while preserving the infraorbital bundle, exposes the anterior surface of the maxilla (-) and the infra-orbital foramen (*)

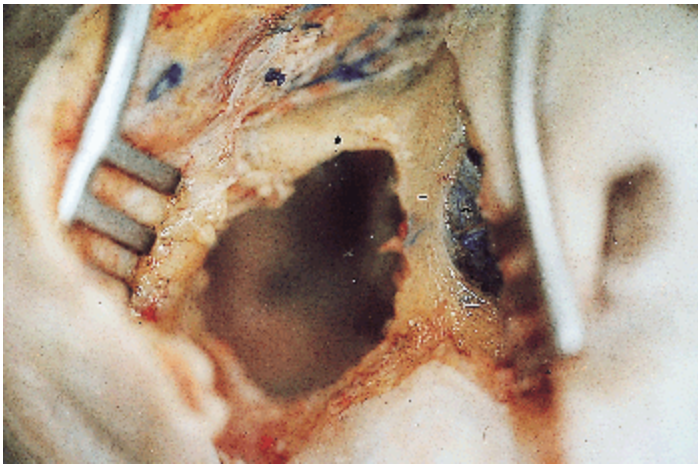


Fig. 4 Anteroposterior view of the anterior maxillotomy (right side). Visualization of the infraorbital bundle. The inferior orbital rim (*), the frontal process of the maxilla (-) and the piriform aperture (^) are spared by the bony resection

Retroantral stage

A wide opening of the lateral part of the posterior maxillary wall of the antrum was performed using Kerrison's rongeurs and high-speed diamond burr drill. This procedure exposed the fatty and arterial retroantral space that corresponded to the anterior part of the ITF. The maxillary a. (MA) was identified, ligated distally, between the origin of the infraorbital and sphenopalatine aa., and divided (Fig. 5). In the upper field, the course of the maxillary n. reaching the foramen rotundum (FR) was followed posteriorly. The infratemporal crest and the root of the lateral pterygoid plate were also exposed.

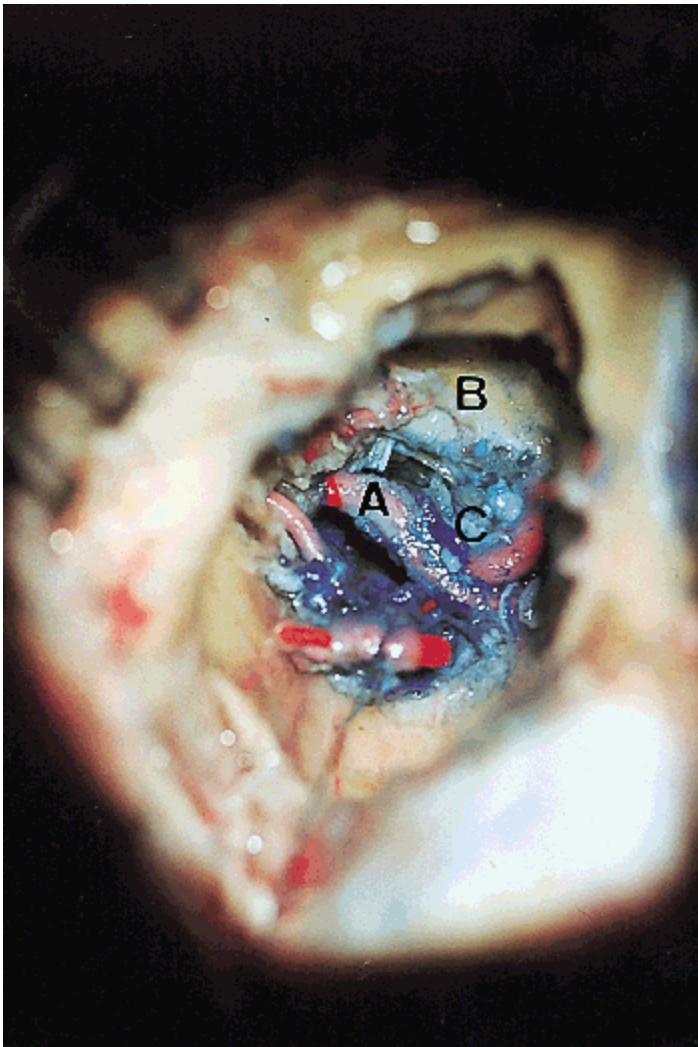


Fig. 5 Anteroposterior view of the posterior maxillotomy (right side), under optic magnification. The retroantral structures are identified, particularly the maxillary a. (*A*), which has been ligated in its distal segment. At the open of the exposure, the maxillary n. reaches the outer meatus of the foramen rotundum (*B*). Observe the rich network of the anterior extension of the pterygoid venous plexus in this specimen (*C*)

Lateropterygoid stage

The lateral pterygoid m. (LPM) occupied this space (Fig. 6) and further access to the foramen ovale (FO) required its extensive desinsertion and partial removal of its superior bundle. This procedure provided identification of the posteromedial compartment of the pterygoid venous plexus (PVP) (Fig. 7) and exposure of the anterolateral margin of the foramen ovale (FO).

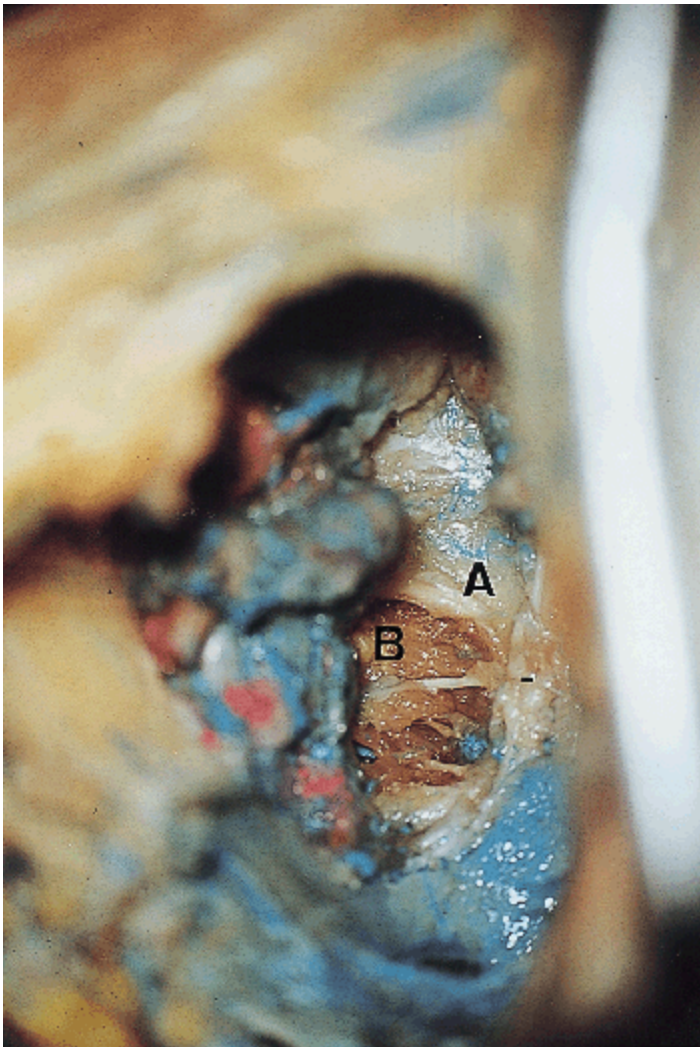


Fig. 6 Anteroposterior view after the lateropterygoid stage (right side), under optic magnification. For better visualization, the maxillary a. has been resected in this specimen. The lateropterygoid space is delineated by the infratemporal crest superiorly (A) and by the lateral pterygoid plate medially. This space is filled by the two heads of the lateral pterygoid m. (B). Anteromedially to the pterygoid process, the sphenopalatine ganglion and the great palatine n. are identified (-)

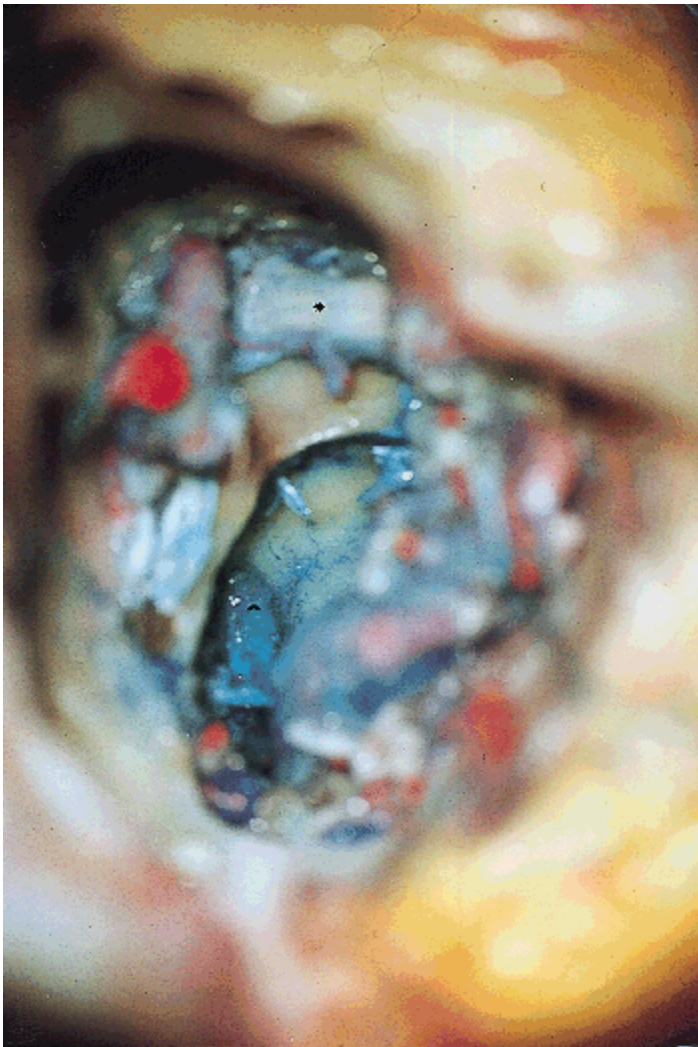


Fig. 7 Anterior view of the latero- and retropterygoid areas (left side) under optic magnification. The lateral pterygoid m. has been dissected and removed. The maxillary n. is identified at the top of the field (*), the pterygoid plate is seen medially. At the lateral margin of the foramen ovale, bridging veins connected to the venous pterygoid plexus are visualized (^). The mandibular n. is hidden by this structure

Measurements between the exposed key structures are given in Table 1. The superficial reference landmark was the meatus of the infra-orbital n. Distances are expressed in mm.

	Mean	Range
d (AW – PW)	38 mm	37-40 mm
d (AW – ML)	39	37-42
d (AW – SC)	41	40-42
d (AW – FR)	44	41-46
d (AW – FO)	56	55-57
d (AW – PP)	41	40-42
d (IC – ML)	9	6-12
w. ASPP	6	4-7
a. V2	31°	28-34°
a. V3	20°	

a. V2, Angle of horizontal exposure of the maxillary branch of the trigeminal n. entering into the foramen rotundum; *a. V3*, angle of horizontal exposure of the mandibular n. entering into the foramen ovale; *AW*, anterior wall of the maxilla; *d*, distance; *FO*, foramen ovale; *FR*, foramen rotundum; *IC*, infratemporal crest of the sphenoid bone; *l. V2*, length of the extracranial portion of the maxillary n. from the infraorbital foramen to the foramen rotundum; *ML*, maxillary a. loop; *mm*, millimetres; *PP*, pterygoid plate; *PW*, posterior wall of the maxilla; *SW*, outer surface of the sphenoid wing; *w. ASPP*, width of the anterior surface of the pterygoid plate

Table 1 Measurements between key structures during the exposure of the ITF via a transmaxillary route

Results

Two subsequent compartments were identified while exposing the ITF via the transmaxillary approach the retroantral space and the lateropterygoid space.

The retroantral space (Fig. 5)

The retroantral space was 5 to 10 mm in anteroposterior depth it was delimited anteriorly by the posterior surface of the maxilla, above by the inferior orbital fissure, and medially by the pterygomaxillary fissure. Posteriorly, this space communicated directly with the lateropterygoid space, and the boundary between them was a virtual coronal plan passing through the infratemporal crest of the sphenoid bone. This space was filled by fat and by a loose venous network extending around the MA. The distal part of the MA, namely the pterygopalatine segment, described a loop, changing from a posteroanterior trajectory to a frontal one, and gave off terminal branches at this level (infraorbital, superior alveolar, sphenopalatine aa.). This loop was in close relation with the thin posterior wall of the antrum and, because of its tortuosity, it could be mobilized easily. The mean height between the sphenoid crest and the artery was 9 mm, ranging from 6 to 12 mm. In its antral course, the infraorbital n. displayed a slight lateromedial and backward trajectory, slightly crossing the top of the field. When exiting from the antrum, it took a sagittal and slightly upward course to reach the anterosuperior surface of the pterygoid process, delineating the entry of the foramen rotundum (FR). Reaching the outer margin of the FR did not exceed a 46-mm depth. The transmaxillary approach allowed a 30° mean exposure of this foramen. Drilling the medial and superior

rim of the FR gave access to the inferior rim of the superior orbital fissure. Our measurements indicated that the pterygopalatine fossa was exposed on a mean 6 mm width in a coronal plan as far as the vertical plate of the palatine bone, medially. In all cases, the pterygopalatine ganglion and palatine n. were identified.

The lateropterygoid space(Fig. 6)

The lateropterygoid space was localized posterior to the retroantral space, lateral to the lateral pterygoid plate and under the greater sphenoid wing. Exposure of this structure via the transmaxillary approach required the use of optic magnification. This space was filled by the LPM. This fleshy muscle ran transversely in the horizontal plane and its two distinct heads, a smaller upper infratemporal and a lower pterygoid one, were clearly exposed. The MA was intimately related to the pterygoid head of the LPM, running lateral to the pterygoid head or between the two bundles. Following the posterior edge of the pterygoid process required a 12 mm additional progression and dissection of the PVP. This plexus was located between the fibers of the LPM and, at its upper surface, connected to the greater sphenoid wing via transosseous channels. In the present study, these multiple venous channels were in the area of the FO. The anterior rim of the FO was reached at a 56 mm mean depth and its inner portion was not totally exposed, concealed by the lateral pterygoid plate. The mean angle of exposure of the FO was 20° in the horizontal plane.

Discussion

The ITF is grossly defined as the anatomic space under the floor of the middle cranial fossa and posterior to the maxilla. The medial wall of the ITF is formed anteriorly by the lateral pterygoid plate and posteriorly by the tensor veli palatini m. The anterior and medial walls are separated superiorly by the pterygomaxillary fissure through which the ITF communicates with the pterygopalatine fossa. The lateral limit of the ITF is the ramus of the mandible. The posterior boundary of the IFT is variously defined. Some authors define it by the prevertebral layer of the cervical fascia and the underlying muscles. This broad definition includes the structures localized behind the styloid mm., including the internal carotid a., internal jugular v. and lower cranial nn. [1, 9]. For other authors, these structures belong to the parapharyngeal space [8]. With them, we define the ITF as the area located below the greater sphenoid wing and where the posterior limit is a plane descending vertically from the sphenosquamosal suture. This is in accordance with the data provided by Robert et al [10], who define this posterior limit by the fascia of the medial pterygoid m. The ITF can be subdivided in a retromaxillozygomatic region, the region of the pterygoid mm. and the pterygopalatine fossa [10]. It may be involved by various pathologic processes and particularly by tumors. Tumors originate primarily from Schwann, vascular, epithelial or mesenchymal tissues of the ITF or involve it secondarily from a neighbouring area. Tumors growing from the parapharyngeal and nasopharyngeal spaces or from the middle cranial fossa are classified in this latter group. To reach those various lesions located in a deep and complex anatomic space, cranial surgeons have developed numerous approaches. In such situations, the appropriate choice of approach is dictated by the origin of the lesion and its exact extension in the IFT. Thus, lesions involving the posterior cranial fossa and invading the ITF are preferentially removed by lateral approaches [4, 11]. Lesions starting in the middle cranial fossa (meningiomas, schwannomas, chordomas, etc.) and secondarily extending into the ITF, are preferentially approached superiorly via a temporal craniotomy. Lesions extending from the parapharyngeal space are exposed after a transmandibular median splitting [6, 8]. In a recent anatomic study, Hitotsumatsu and Rhoton [5] described various combinations of subtotal maxillectomies in order to expose the totality of the elements of the infratemporal fossa. Traditionally, approaches of the ITF can also be classified as extensive for carcinologic surgery, or minimally invasive if the aim is a simple exploration or biopsy. Nevertheless, recent refinements of imaging techniques have reduced the role of exploratory surgery and, in order to minimize cosmetic and functional morbidity, surgeons nowadays attempt to perform, if possible, tumor removal via conservative routes. Using the natural space offered by air cavities, the transmaxillary approach appears to be a safe and simple procedure. It preserves the functional anatomy of the nose and allows the initial control of the neurovascular structures, namely the infraorbital n. and the MA. The infraorbital n. course is used as a guide during anteroposterior progression in the antrum. Careful opening of the posterior wall of the antrum avoids the risk of MA bleeding. This serpentine artery is enclosed in a sheath of venous network that can be dissected without problems. Mobilization and sometimes ligation and section of this artery are required to progress deeper into the ITF. Vrionis et al [12] demonstrated that the tortuous feature of this artery could allow tension-free in situ anastomosis to the supraclinoid part of the carotid a. when using temporal craniotomy.

Some limitations of this approach can be deduced from the present study. A sublabial incision appeared to be insufficient for exposure of the anterior surface of the maxilla and puts the infraorbital n. at risk of traction injury. Moreover, it is broadly admitted that the required paralateronasal skin incision is cosmetically acceptable. As shown by our measurements, this route is deep and narrow for exposure of structures located posterior to the plane of the pterygoid process. Thus, delineation of the boundaries of the FO is allowed only by a 20° angle of vision at more than 55 mm depth. The reduced exposure of this foramen is additionally due to its outer masking by the lateral pterygoid plate. Moreover, two major structures reduce the access to the retropterygoid region. In all cadavers, we have seen that the LPM tightly filled the lateropterygoid space. By the transmaxillary route, single retraction of this fleshy muscle was not possible and further progress required desinsertion and resection of its superior bundle. The other important obstacle is the complex anatomy and density of the PVP. A recent

anatomic study [3] showed that, in most specimens, the PVP was organised in an anterolateral compartment connected with the deep facial v., and a posteromedial compartment connected with the middle cranial fossa. Indeed, we always encountered this latter venous network under the greater sphenoid wing, receiving multiple emissary vv. from the parasellar region. Behind this plexus was condensed in the area of the FO. This approach can be widened by an adjunctive Lefort I maxillotomy [7]. This procedure provides a gain of 10 mm in height at the retroantral stage but does not correct the narrow horizontal angle of vision of the retropterygoid elements. Moreover, it significantly increases the morbidity, because of the possible occurrence of bone necrosis, loss of dental viability and hemorrhage.

Conclusions

The results of the present anatomic study show that the transmaxillary route is a minimally invasive route convenient to expose the structures of the anterior part of the ITF, including the retroantral area, pterygomaxillary fissure and pterygopalatine fossa. By this route, the entire extracranial portion of the maxillary n. is safely exposed. Likewise, lesions involving the orbital roof and the inferior orbital fissure also can be extirpated while preserving the maxillary n. Assuming retraction of the LPM, small and circumscribed lesions involving the lateropterygoid area can also be reached via this deep but direct corridor. Conversely, management of lesions involving the area of the FO cannot be achieved easily because of the reduced angle of exposure and the depth of the dissection. These obstacles could be overcome by additional muscular removal and bone drilling.

Acknowledgments We are grateful to Stéphane Sourice for laboratory and photographic assistance.

References

1. Bejjani GK, Sullivan B, Salas-Lopez DC, Abello J, Wright DC, Jurjus A, Sekhar LN (1998) Surgical anatomy of the infratemporal fossa The styloid diaphragm revisited. *Neurosurgery* 43 842-853
2. Couldwell WT, Sabit I, Weiss MH, Giannotta SL, Rice D (1997) Transmaxillary approach to the anterior cavernous sinus a microanatomic study. *Neurosurgery* 40 1307-1311
3. Deplus S, Bremond-Gignac D, Gillot C, Lassau JP (1996) The pterygoid venous plexuses. *Surg Radiol Anat* 18 23-27
4. Fisch U (1978) Infratemporal fossa approach to tumors of the temporal bone and base of the skull. *J Laryngol Otol* 92 949-967
5. Hitotsumatsu T, Rhoton AL (2000) Unilateral upper and lower subtotal maxillectomy approaches to the cranial base microsurgical surgery. *Neurosurgery* 46 1416-1453
6. Legent F, Laccourreye H (1991) La fosse infratemporale. Arnette, Paris, pp 195-203
7. Moloney F, Worthington P (1981) The origin of the Le Fort I maxillary osteotomy. Cheever's operation. *J Oral Surg* 39 731-734
8. Olsen KD (1994) Tumors and surgery of the parapharyngeal space. *Laryngoscope* 104 [suppl. 63] 1-28
9. Pellet W, Cannoni M, Pech A (1989) *Oto-Neuro-Chirurgie*. Springer-Verlag, Paris, pp 55-58
10. Robert R, Legent F, Rogez JM, Menier Y, Hérouy Y, Patra P, Leborgne J (1989) The infratemporal fossa A trial classification. *Surg Radiol Anat* 11 307-311
11. Sekhar LN, Schramm VL, Jones NF (1987) Subtemporal-preauricular infratemporal fossa approach to large lateral and posterior cranial base neoplasms. *J Neurosurg* 67 488-499
12. Vrionis FD, Cano WG, Heilman CB (1996) Microsurgical anatomy of the infratemporal fossa as viewed laterally and superiorly. *Neurosurgery* 39 777-786

